

Evidence for a charged charmonium-like Z_c^+ from QCD

Sasa Prelovsek^{*a,b}, C. B. Lang^{†c}, Luka Leskovec^{‡b}, and Daniel Mohler^{§d}

^a*Department of Physics, University of Ljubljana, 1000 Ljubljana, Slovenia*

^b*Jozef Stefan Institute, 1000 Ljubljana, Slovenia*

^c*Institute of Physics, University of Graz, A-8010 Graz, Austria*

^d*Fermi National Accelerator Laboratory, P.O. Box 500, Batavia, Illinois 60510-5011, USA*

Abstract

Recently experimentalists have discovered a new state of matter in form of charged charmonium-like hadrons Z_c^+ . Unlike conventional hadrons, these contain at least two valence quarks and two antiquarks ($\bar{c}c\bar{d}u$). We address the question whether the existence of such a new form of hadrons is supported by QCD via a first-principle calculation using Lattice QCD. We find a candidate for the charged charmonium-like state Z_c^+ with quantum numbers $I^G(J^{PC}) = 1^+(1^{+-})$. This is the first ab-initio QCD calculation establishing such a hadron. The state is found at mass $m = 4.16 \pm 0.03 \pm 0.16 \pm \mathcal{O}(\Gamma_{Z_c})$ GeV and could be related to the recently discovered $Z_c^+(4020)/Z_c^+(4025)$ or $Z_c^+(4200)$. The Z_c^+ candidate emerges only when diquark-antidiquark creation operators are included in the simulation. The resulting overlap of the established Z_c^+ to our basis of creation operators \mathcal{O}_j may shed light on its nature.

*sasa.prelovsek@ijs.si

†christian.lang@uni-graz.at

‡luka.leskovec@ijs.si

§dmohler@fnal.gov

Quantum Chromodynamics (QCD) is the fundamental quantum field theory of quarks and gluons. In its strong coupling regime it should explain the masses and other properties of hadrons. Conventional hadrons are composed of either a valence quark q and antiquark \bar{q} (mesons) or three valence quarks (baryons) on top of the sea of quark-antiquark pairs and gluons. One of the most notable and perhaps surprising features until recently was the complete absence of exotic hadrons like $\bar{q}\bar{q}qq$ or $\bar{q}qqqq$.

This has changed due to fascinating experimental discoveries over the past seven years. Most of the newly discovered exotic states have unconventional flavor content, likely $\bar{c}c\bar{d}u$, and spin and parity quantum numbers $J^P = 1^+$:

- $Z^+(4430)$, discovered in 2007 by Belle [1], unconfirmed by BaBar [2], in 2014 confirmed by LHCb [3] giving $J^P = 1^+$.
- $Z_c^+(3900)$ slightly above $D\bar{D}^*$ threshold; discovered in the $J/\psi\pi^+$ invariant mass by BESIII [4], confirmed by Belle [5] and using CLEO-c data [6]; spin and parity unclear; may correspond to the same state as $Z_c^+(3885) \rightarrow (D\bar{D}^*)^+$ with known $J^P = 1^+$ [7].
- $Z_c^+(4020) \rightarrow h_c\pi^+$ [8] and $Z_c^+(4025) \rightarrow (D^*\bar{D}^*)^+$ [9] discovered by BESIII slightly above $D^*\bar{D}^*$ threshold; may correspond to the same state, spin and parity unclear but $J^P = 1^+$ preferred.
- $Z^+(4200) \rightarrow J/\psi\pi^+$ reported in 2014 by Belle [10] favoring $J^P = 1^+$.

All these states have G-parity $G = +1$ while their neutral partners have charge conjugation $C = -1$. Therefore we focus on the channel with $I^G(J^{PC}) = 1^+(1^{+-})$.

On the theoretical side, the existence of such states is not yet settled within QCD. While these states have been addressed theoretically with a number of phenomenological approaches like quark models, (unitarized) effective field theory and QCD sum rules (for reviews with references see [11, 12, 13]), these approaches are not based directly on QCD or they depend on parameters (i.e., low energy constants) that are not present in the QCD Lagrangian. The existence of Z_c^+ has never been established from first-principle QCD. The problem is a large magnitude of the strong coupling constant α_s at the hadronic energy scale, hence a perturbative expansion is not successful. Lattice QCD represents the only non-perturbative approach that is based directly on QCD, depending only on parameters m_q and α_s that appear in the QCD Lagrangian. It consists of the numerical evaluation of the corresponding Feynman path integrals on a discretized and finite Euclidean space-time lattice of size $L^3 \times T$ with lattice spacing a .

Therefore it is an urgent theoretical task to establish whether QCD supports the presence of an exotic state with quark content $\bar{c}c\bar{d}u$ using *ab-initio* lattice QCD simulations. Here we undertake this task and search for candidates with mass below 4.3 GeV. The principal aim of the present study is not to determine the nature of Z_c^+ , which would entail discriminating between various possibilities such as mesonic molecules, diquark-antidiquark structures, hadrocharmonium [14] or Born-Oppenheimer tetraquarks [15]; the goal is rather to establish whether such a state exists in QCD or not. Nevertheless the overlaps $\langle \Omega | \mathcal{O}_j | Z_c^+ \rangle$ of the established Z_c^+ candidate to our lattice creation operators \mathcal{O}_j shed some light on its nature.

Energy eigenstates on a finite lattice

In lattice QCD simulations the states are identified from discrete energy-levels E_n and in principle all physical eigenstates with given quantum numbers appear. The eigenstate of interest, Z_c^+ , gives an energy level at $E_n \simeq m_{Z_c}$ if it exists. However, various two-meson states $M_1(\mathbf{p})M_2(-\mathbf{p})$ have the same quantum numbers and are also physical eigenstates, which presents a major challenge. Individual momenta are discretized due to the periodic boundary conditions in space. If the two mesons do not interact, then $\mathbf{p} = \frac{2\pi}{L}\mathbf{k}$ with $\mathbf{k} \in \mathbb{N}^3$, and the energies of $M_1(k)M_2(-k)$ states are

$$E^{n.i.} = E_1(k) + E_2(k) \quad \text{with} \quad E_{1,2}(k) = \sqrt{m_{1,2}^2 + k(\frac{2\pi}{L})^2}. \quad (1)$$

These values are slightly shifted in presence of the interaction. In experiment, these states correspond to the two-meson decay products with a continuous energy spectrum.

Our simulation employs dynamical u and d quarks that correspond to the pion mass $m_\pi \simeq 266$ MeV [16, 17]. The rather small box $L^3 \times T$ with $L \simeq 2$ fm is responsible for crucial practical advantages, detailed in the Supplementary Material. On this lattice, the two-particle states with $I^G(J^P) = 1^+(1^+)$ and total momentum zero in the energy region of interest $E \leq 4.3$ GeV are

$$\begin{aligned} & J/\psi(0)\pi(0), \quad \eta_c(0)\rho(0), \quad J/\psi(1)\pi(-1), \quad D(0)\bar{D}^*(0), \quad \psi_{2S}(0)\pi(0), \\ & D^*(0)\bar{D}^*(0), \quad \psi_{3770}(0)\pi(0), \quad D(1)\bar{D}^*(-1), \quad \psi_3(0)\pi(0) \end{aligned} \quad (2)$$

in order of increasing energy. Their lattice energies $E^{n.i.}$ in the non-interacting limit are denoted by the horizontal lines in Fig. 1b and the values follow from the masses and single-meson energies determined on the same set of gauge configurations [16, 18]. The appearance of $\psi_3\pi$, where ψ_3 denotes the charmonium with $J^{PC} = 3^{--}$, is an artifact due to finite a as discussed in Supplementary Material. The $h_c(0)\pi(0)$ is not present for $J^P = 1^+$ since non-vanishing relative momentum p is required by the orbital momentum $l = 1$.

Our aim is to extract and identify all two-particle energy-levels (2) from the full, coupled correlation matrix of hadron operators and establish whether QCD predicts additional states. An additional state would imply the existence of an exotic Z_c^+ hadron. This goal presents a considerable challenge by itself. Note that a rigorous treatment (via a Lüscher-type finite volume formalism [19, 20, 21, 22, 23]) would require the determination of the scattering matrix for all two-particle channels that couple, and a subsequent determination of the mass and the width for any Z_c^+ resonance(s). This is beyond capabilities of any lattice simulation at present or in the near future. Therefore we take a simplified approach where the existence of Z_c^+ is established by analyzing the number of energy levels, their positions and overlaps with the considered lattice operators $\langle \Omega | \mathcal{O}_j | n \rangle$. We point out that the rigorous formalism does predict an appearance of a level in addition to the (shifted) two-particle levels if there is a relatively narrow resonance.

Previous lattice simulations

The first lattice simulation aimed at $Z_c^+(3900)$ focused on the region below 4 GeV and found only two-particle states and no indication for $Z_c^+(3900)$ [24]. The second simulation studied $D\bar{D}^*$ scattering near threshold in the same channel and did not yield any indication for $Z_c^+(3900)$ either [25].

Calculational Method

The energies E_n and the overlaps Z_j^n of the physical eigenstates n are extracted from the correlation matrix

$$C_{jk}(t) = \langle \Omega | \mathcal{O}_j(t_{src} + t) \mathcal{O}_k^\dagger(t_{src}) | \Omega \rangle = \sum_n Z_j^n Z_k^{n*} e^{-E_n t}, \quad Z_j^n \equiv \langle \Omega | \mathcal{O}_j | n \rangle, \quad j, k = 1, \dots, 18. \quad (3)$$

The physical system for given quantum numbers is created from the vacuum $|\Omega\rangle$ using creation operators \mathcal{O}_k^\dagger at time t_{src} and the system propagates for time t before being annihilated at t_{sink} by \mathcal{O}_j . The creation/annihilation operators are called interpolators. The right-hand side (3) is obtained by means of spectral decomposition after $I = \sum_n |n\rangle\langle n|$ is inserted.

We employ fourteen interpolators $O^{M_1 M_2}$ that couple well to the two-particle states (2) and add diquark-antidiquark interpolators \mathcal{O}^{4q} which may be important for the exotic state Z_c^+ . A full description of our interpolators is given in the Supplementary Material.

The Wick contractions for the matrix of correlators (3) with $I=1$ involve only diagrams where the light quarks \bar{d} and u propagate from source to sink. Concerning charm quarks, there are diagrams where they propagate from source to sink and diagrams where charm quarks annihilate (Fig. 4 of the Supplementary Material). The second class represents mixing with channels that contain no charm quarks, their effect is suppressed due to the Okubo-Zweig-Iizuka rule, and the experiments do not observe these decay channels in the region of interest. The results in the present work are therefore based on all contractions where charm quarks propagate from source to sink (Fig. 4a of the Supplementary Material).

The energies E_n and overlaps Z_j^n are obtained from the 18×18 correlation matrix (3) using the generalized eigenvalue method [26, 27, 28, 29]. We solve $C(t)u^{(n)}(t) = \lambda^{(n)}(t)C(t_0)u^{(n)}(t)$ for the eigenvalues and eigenvectors and extract the energies E_n from the asymptotically exponential behaviour of the eigenvalues: $\lambda^{(n)}(t) \propto e^{-E_n t}$ at large t . We use correlated two-exponential fits to $\lambda^{(n)}(t)$ and find consistent results for $t_0 = 2, 3$ and we present them for $t_0 = 2$. Overlap factors follow from

$$Z_j^{(n)}(t) = e^{E_n t/2} \frac{|C_{jk}(t)u_k^{(n)}(t)|}{|C(t)^{\frac{1}{2}}u^{(n)}(t)|}, \quad (4)$$

fitted to a constant in $7 \leq t \leq 10$.

The treatment of the charm quarks requires special care due to discretization errors. We employ the Fermilab method [30], where discretization uncertainties are suppressed in the difference $E_n - m_{s.a.}$ with the spin-average mass $m_{s.a.} \equiv \frac{1}{4}(m_{\eta_c} + 3m_{J/\psi})$. The same method

and tuning of the charm quark mass m_c lead to a good agreement with experiment for conventional charmonium [16], masses and widths of D mesons [16], and the D_s spectrum [31, 17] on this ensemble. In view of this, we will compare $E_n^{lat} - m_{s.a.}^{lat} + m_{s.a.}^{exp}$ to experiment where $am_{\eta_c}^{lat} = 1.47392(31)$ and $am_{J/\psi}^{lat} = 1.54171(43)$.

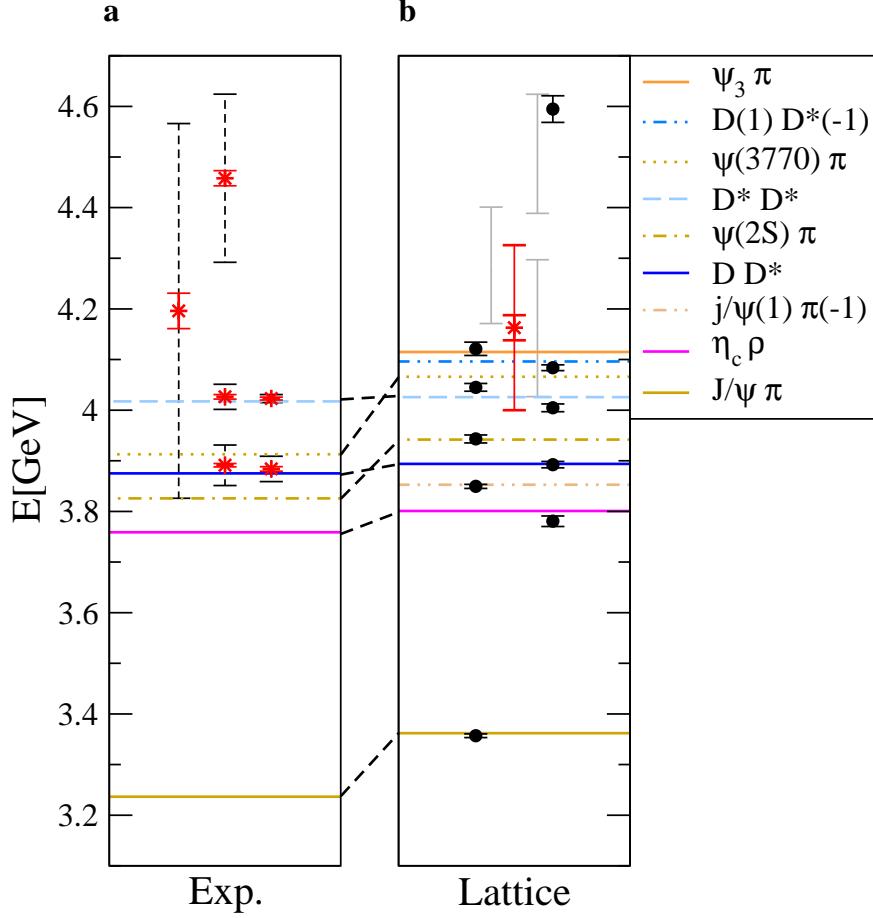


Figure 1: **The spectrum for quantum numbers $I^G(J^{PC}) = 1^+(1^{+-})$.** **a** position of the experimental Z_c^+ candidates [11]; **b** the discrete energy spectrum from our lattice simulation. The horizontal lines represent energies of the non-interacting two-particle states (2) with $E \leq 4.3$ GeV on our lattice. The nine lowest lattice energy levels (black circles) are interpreted as two-particle states, which are inevitably present in a dynamical lattice QCD simulation. The grayed out energy levels cannot be reliably extracted but indicate some overlap of our basis with states between 4.1 and 4.7 GeV. From their composition it is unlikely that these are exotic state candidates. The additional energy level indicated by the red asterisk is our candidate for the exotic Z_c^+ . The larger error bar on the red asterisk combines statistical and systematic uncertainties, while all other lattice errors are statistical only. The experimental widths of the resonances are indicated by the dashed vertical lines.

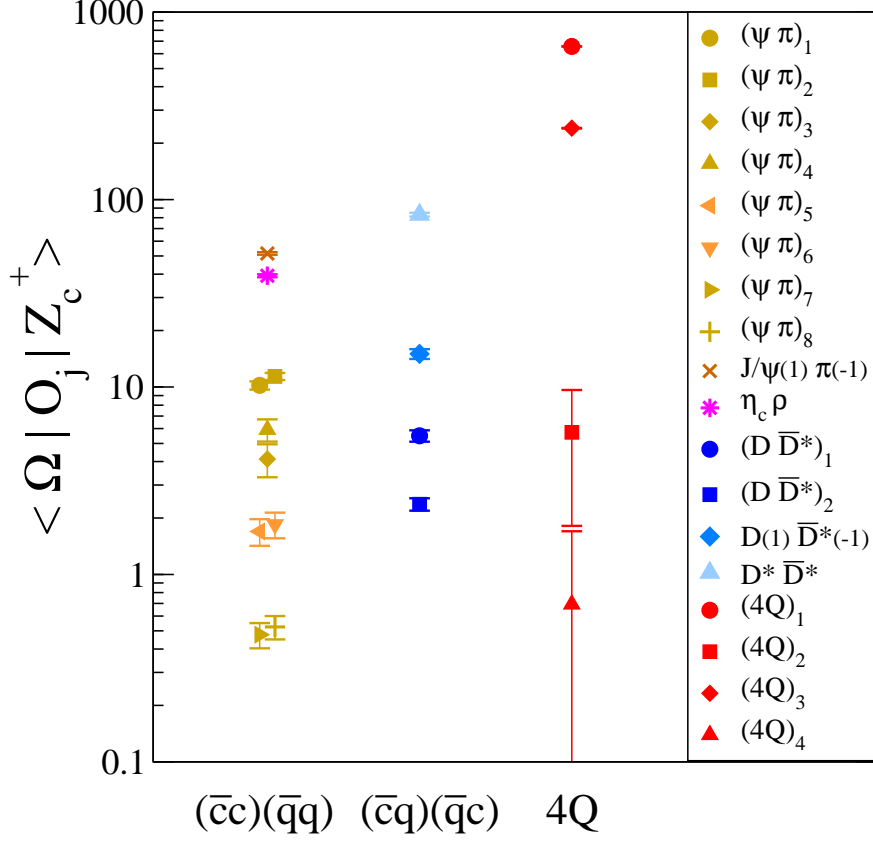


Figure 2: **Composition of Z_c^+** . The overlaps $\langle \Omega | \mathcal{O}_j | Z_c^+ \rangle$ show how our candidate for Z_c^+ with $E \simeq 4.16$ GeV couples to the vacuum Ω via the employed creation operators \mathcal{O} (listed in Supplementary Material).

Results

The central result of our simulation is the discrete spectrum in Fig. 1b, while experimental candidates in the same channel are collected in Fig. 1a. In the energy region below $E \leq 4.3$ GeV one expects nine discrete two-particle states (2) near the horizontal lines, which continue in Fig. 1a to show their relation to the continuum of scattering states in experiment. However, we clearly observe ten energy levels with $E \leq 4.3$ GeV and therefore one of them is a candidate for the exotic Z_c^+ .

We identify level $n = 10$ with $E \simeq 4.16$ GeV as the Z_c^+ candidate (indicated by the red asterisk) for the following reasons. First, the diquark-antidiquark interpolating fields \mathcal{O}^{4q} are crucial for the existence of this level. This is illustrated in Fig. 3c, which presents the spectrum if \mathcal{O}_{1-4}^{4q} are excluded: the lowest nine levels remain unaffected and level ten disappears. Second, the level $n = 10$ has the largest overlap with $\mathcal{O}_{1,3}^{4q}$ and smaller overlaps with $O^{M_1 M_2}$, as shown in Fig. 2. Third, level $n = 10$ has a larger overlap with \mathcal{O}_1^{4q} than the remaining levels n (see Supplementary Material).

We interpret the lowest nine levels as (interacting) two-particle states since they appear very near the non-interacting energies (1) of the two-particle states (2). Each of them has the biggest overlap with the corresponding $\mathcal{O}^{M_1 M_2}$, as shown in Fig. 5 of the Supplementary Material. When either one of $\mathcal{O}^{D^{(0)}D^{*(0)}}$, $\mathcal{O}^{D^{(1)}D^{*(-1)}}$, $\mathcal{O}^{\psi(1)\pi(-1)}$ or $\mathcal{O}^{D^{*(0)}D^{*(0)}}$ are omitted from the correlation matrix, the corresponding two-particle level disappears from the spectrum (Figs. 3d-g). This indicates that these two-particle states are either decoupled or cannot be reliably extracted for the basis without the corresponding interpolators.

The Z_c^+ established in this work has the mass $m_{Z_c} = E_{10} - m_{s.a.}^{lat} + m_{s.a.}^{exp}$, i.e.

$$m_{Z_c} = 4.16 \pm 0.03 \pm 0.16 \pm \mathcal{O}(\Gamma_{Z_c}) \text{ GeV} , \quad (5)$$

where the first error is statistical and determined using single-elimination jackknife. The second and third uncertainties are estimated bounds for the systematic error which need some discussion. The second uncertainty consists of adding estimates for uncertainties from $m_{u,d}$ dependence, charm quark discretization effects and possible scale setting ambiguities in quadrature. In absence of a rigorous framework for the $m_{u,d}$ dependence of Z_c^+ (which does contain valence $\bar{d}u$ quarks) our upper bound for the associated uncertainty is $m_\pi - m_\pi^{phy} \simeq 0.13$ GeV. This corresponds to both, the mass dependence of the pion itself and approximately to the mass dependence of the fastest moving threshold in the system. Typical charm quark discretization errors are of the same size as in Fig. 3 of [32] and we expect them to add up to no more than 70 MeV for $E_{10} - m_{s.a.} \simeq 1.1$ GeV. The ambiguity from our scale setting procedure to m_{Z_c} is expected to be below 50 MeV. This combination results in a systematic uncertainty of 0.16 GeV. The uncertainty from volume effects can be of order $\pm\Gamma_Z$ for a Z_c with hadronic width Γ_{Z_c} and only extracting phase shifts and inelasticities in the coupled channel system can resolve this uncertainty.

This QCD result supports the existence of an exotic Z_c^+ . The resulting mass (5) indicates that the established state can be related to the relatively narrow $Z_c^+(4020)$ or $Z_c^+(4025)$ observed slightly above $D^*\bar{D}^*$ threshold by BESIII [8, 9]. Our Z_c^+ also lies close above the $D^*\bar{D}^*$ threshold (Fig. 1b) and the overlap of Z_c^+ to $\mathcal{O}^{D^*D^*}$ is largest among all $\mathcal{O}^{M_1 M_2}$. The second possibility is to relate Z_c^+ (5) with the broad state $Z^+(4200)$ observed by Belle [10]. A relation of Z_c^+ (5) with the observed $Z_c^+(3895)/Z_c^+(3900)$ [4, 5, 6, 7] is less likely in view of its mass.

We refrain from associating a specific structure such as mesonic molecule, diquark-antidiquark, hadrocharmonium [14] or Born-Oppenheimer tetraquark [15] with the observed Z_c hadron. The overlaps of the resulting state with the employed interpolating fields in Fig. 2 however suggest that $\mathcal{O}_{1,3}^{4q}$ and $\mathcal{O}^{D^*D^*}$ play a particularly important role.

The ground state for the quantum numbers in our study is $J/\psi\pi$ and we observe it for most interpolators at large t , also for \mathcal{O}^{4q} . Looking at the ground state of the diquark-antidiquark correlators only, one cannot reach conclusions regarding Z_c^+ . This holds also for the ground states from \mathcal{O}^{DD^*} (used in [25]) or $\mathcal{O}^{D^*D^*}$ correlators alone. The coupling to $J/\psi\pi$, $\eta_c\rho$ (and possibly some others) has to be taken into account, as shown by our study. These cautionary remarks also apply to QCD sum-rule studies that are based on correlators. A lattice study for larger volumes will involve even more physical states $M_1(k)M_2(-k)$ and thus need further operators, a highly challenging task.

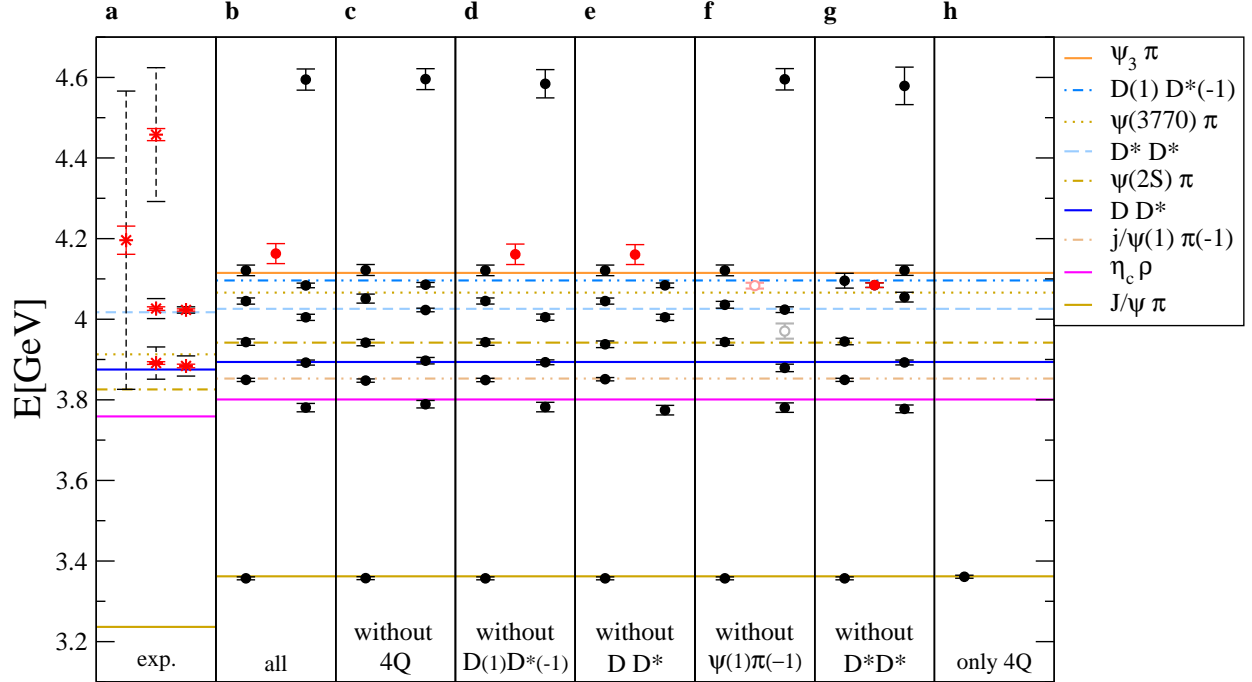


Figure 3: **The spectrum in the channel $I^G(J^{PC}) = 1^+(1^{+-})$.** **a,b** same as in Fig. 1, where the lattice spectrum is based on the full 18×18 correlation matrix; **c** shows the lattice spectrum based on the 14×14 correlation matrix without diquark-antidiquark interpolating fields \mathcal{O}_{1-4}^{4q} ; spectra **d-g** are based on truncated correlation matrices as described in the figure; spectrum **h** is based on \mathcal{O}_{1-4}^{4q} only. The horizontal lines represent energies of the non-interacting two-particle states (2). Statistical errors on the lattice spectrum are shown.

Conclusions

Our ab-initio QCD calculation provides evidence for the existence of an exotic Z_c^+ . We find a candidate for a state with a flavor content $\bar{c}c\bar{d}u$ and quantum numbers $I^G(J^{PC}) = 1^+(1^{+-})$ at a mass $m = 4.16 \pm 0.03 \pm 0.16 \pm \mathcal{O}(\Gamma_{Z_c})$ GeV. It could be related to $Z_c^+(4020)/Z_c^+(4025)$ recently discovered by BESIII or to $Z_c^+(4200)$ found by Belle. Our result further confirms that the simple classification of hadrons into $\bar{q}q$ mesons and qqq baryons has to be revisited.

Acknowledgments

We thank Anna Hasenfratz for providing the gauge configurations. S.P. thanks Changzheng Yuan and Anže Zupanc for discussion and D.M. is grateful for discussions with Jim Simone. We acknowledge the support by the Slovenian Research Agency ARRS project N1-0020 and by the Austrian Science Fund FWF project I1313-N27. Fermilab is operated by Fermi Research Alliance, LLC under Contract No. De-AC02-07CH11359 with the United States Department of Energy.

References

- [1] Choi, S. *et al.* Observation of a resonance-like structure in the $\pi^+\pi^-\psi'$ mass distribution in exclusive $B \rightarrow K\pi^+\pi^-\psi'$ decays. *Phys. Rev. Lett.* **100**, 142001 (2008). [arXiv:0708.1790](#).
- [2] Aubert, B. *et al.* Search for the $Z(4430)^-$ at BABAR. *Phys. Rev.* **D79**, 112001 (2009). [arXiv:0811.0564](#).
- [3] Aaij, R. *et al.* Observation of the resonant character of the $Z(4430)^-$ state (2014). [arXiv:1404.1903](#).
- [4] Ablikim, M. *et al.* Observation of a Charged Charmoniumlike Structure in $e^+e^- \rightarrow \pi^+\pi^-J/\psi$ at $\sqrt{s}=4.26\text{GeV}$. *Phys. Rev. Lett.* **110**, 252001 (2013). [arXiv:1303.5949](#).
- [5] Liu, Z. *et al.* Study of $e^+e^- \rightarrow \pi^+\pi^-J/\psi$ and Observation of a Charged Charmoniumlike State at Belle. *Phys. Rev. Lett.* **110**, 252002 (2013). [arXiv:1304.0121](#).
- [6] Xiao, T., Dobbs, S., Tomaradze, A. & Seth, K. K. Observation of the Charged Hadron $Z_c^\pm(3900)$ and Evidence for the Neutral $Z_c^0(3900)$ in $e^+e^- \rightarrow \pi\pi J/\psi$ at $\sqrt{s} = 4170$ MeV. *Phys. Lett.* **B727**, 366–370 (2013). [arXiv:1304.3036](#).
- [7] Ablikim, M. *et al.* Observation of a charged $(D\bar{D}^*)^-$ mass peak in $e^+e^- \rightarrow \pi^+(D\bar{D}^*)^-$ at $E_{\text{cm}}=4.26$ GeV. *Phys. Rev. Lett.* **112**, 022001 (2014). [arXiv:1310.1163](#).
- [8] Ablikim, M. *et al.* Observation of a charged charmoniumlike structure $Z_c(4020)$ and search for the $Z_c(3900)$ in $e^+e^- \rightarrow \pi^+\pi^-h_c$. *Phys. Rev. Lett.* **111**, 242001 (2013). [arXiv:1309.1896](#).
- [9] Ablikim, M. *et al.* Observation of a charged charmoniumlike structure in $e^+e^- \rightarrow (D^*\bar{D}^*)^\pm\pi^\mp$ at $\sqrt{s} = 4.26\text{GeV}$. *Phys. Rev. Lett.* **112**, 132001 (2014). [arXiv:1308.2760](#).
- [10] Chilikin, K. Recent results on quarkonium(-like) states at Belle (talk given at Rencontres de Moriond QCD and High Energy Interactions, La Thuile, March 22 - 29, 2014). <http://moriond.in2p3.fr/QCD/2014/MondayAfternoon/Chilikin.pdf>
- [11] Brambilla, N. *et al.* QCD and strongly coupled gauge theories: challenges and perspectives (2014). [arXiv:1404.3723](#).
- [12] Brambilla, N. *et al.* Heavy quarkonium: progress, puzzles, and opportunities. *Eur. Phys. J.* **C71**, 1534 (2011). [arXiv:1010.5827](#).
- [13] Liu, X. An overview of XYZ new particles (2013). [arXiv:1312.7408](#).
- [14] Voloshin, M. $Z_c(3900)$ - what is inside? *Phys. Rev.* **D87**, 091501 (2013). [arXiv:1304.0380](#).

- [15] Braaten, E. How the $Z_c(3900)$ Reveals the Spectra of Quarkonium Hybrid and Tetraquark Mesons. *Phys. Rev. Lett.* **111**, 162003 (2013). [arXiv:1305.6905](#).
- [16] Mohler, D., Prelovsek, S. & Woloshyn, R. M. $D\pi$ scattering and D meson resonances from lattice QCD. *Phys. Rev.* **D87**, 034501 (2013). [arXiv:1208.4059](#).
- [17] Lang, C. B., Leskovec, L., Mohler, D., Prelovsek, S. & Woloshyn, R. M. D_s mesons with DK and D^*K scattering near threshold (2014). [arXiv:1403.8103](#).
- [18] Lang, C. B., Mohler, D., Prelovsek, S. & Vidmar, M. Coupled channel analysis of the ρ meson decay in lattice QCD. *Phys. Rev.* **D84**, 054503 (2011). [arXiv:1105.5636](#).
- [19] Lüscher, M. Volume Dependence of the Energy Spectrum in Massive Quantum Field Theories. 2. Scattering States. *Commun. Math. Phys.* **105**, 153–188 (1986).
- [20] Lüscher, M. Two particle states on a torus and their relation to the scattering matrix. *Nucl. Phys.* **B354**, 531–578 (1991).
- [21] Döring, M., Meissner, U.-G., Oset, E. & Rusetsky, A. Unitarized Chiral Perturbation Theory in a finite volume: Scalar meson sector. *Eur. Phys. J.* **A47**, 139 (2011). [arXiv:1107.3988](#).
- [22] Hansen, M. T. & Sharpe, S. R. Multiple-channel generalization of Lellouch-Lüscher formula. *Phys. Rev.* **D86**, 016007 (2012). [arXiv:1204.0826](#).
- [23] Briceño, R. A. Two-particle multichannel systems in a finite volume with arbitrary spin. *Phys. Rev.* **D89**, 074507 (2014). [arXiv:1401.3312](#).
- [24] Prelovsek, S. & Leskovec, L. Search for $Z_c^+(3900)$ in the 1^{+-} Channel on the Lattice. *Phys. Lett.* **B727**, 172–176 (2013). [arXiv:1308.2097](#).
- [25] Chen, Y. *et al.* Low-energy Scattering of $(D\bar{D}^*)^\pm$ System And the Resonance-like Structure $Z_c(3900)$ (2014). [arXiv:1403.1318](#).
- [26] Michael, C. Adjoint Sources in Lattice Gauge Theory. *Nucl. Phys.* **B259**, 58 (1985).
- [27] Lüscher, M. Volume Dependence of the Energy Spectrum in Massive Quantum Field Theories. 1. Stable Particle States. *Commun. Math. Phys.* **104**, 177 (1986).
- [28] Lüscher, M. & Wolff, U. How to Calculate the Elastic Scattering Matrix in Two-dimensional Quantum Field Theories by Numerical Simulation. *Nucl. Phys.* **B339**, 222–252 (1990).
- [29] Blossier, B., Della Morte, M., von Hippel, G., Mendes, T. & Sommer, R. On the generalized eigenvalue method for energies and matrix elements in lattice field theory. *JHEP* **0904**, 094 (2009). [arXiv:0902.1265](#).

- [30] El-Khadra, A. X., Kronfeld, A. S. & Mackenzie, P. B. Massive fermions in lattice gauge theory. *Phys. Rev.* **D55**, 3933–3957 (1997). [arXiv:hep-lat/9604004](#).
- [31] Mohler, D., Lang, C. B., Leskovec, L., Prelovsek, S. & Woloshyn, R. M. $D_{s_0}^*$ (2317) Meson and D -Meson-Kaon Scattering from Lattice QCD. *Phys. Rev. Lett.* **111**, 222001 (2013). [arXiv:1308.3175](#).
- [32] Oktay, M. B. & Kronfeld, A. S. New lattice action for heavy quarks. *Phys. Rev.* **D78**, 014504 (2008). [arXiv:0803.0523](#).
- [33] Dudek, J. J., Edwards, R. G., Mathur, N. & Richards, D. G. Charmonium excited state spectrum in lattice QCD. *Phys. Rev.* **D77**, 034501 (2008). [arXiv:0707.4162](#).
- [34] Peardon, M. *et al.* A Novel quark-field creation operator construction for hadronic physics in lattice QCD. *Phys. Rev.* **D80**, 054506 (2009). [arXiv:0905.2160](#).

Supplementary material to

“Evidence for a charged charmonium-like state Z_c^+ from QCD”

Details of the simulation

The simulation is based on one ensemble of gauge configurations with Clover-Wilson dynamical quarks, and the same type of valence u, d quarks. Their masses satisfy $m_u = m_d$, $m^{val} = m^{dyn}$ and correspond to $m_\pi = 266(4)$ MeV. The lattice spacing is $a = 0.1239(13)$ fm, the volume is $V = 16^3 \times 32$ and the spatial size $L \simeq 2$ fm. A rather small L may lead to sizable finite volume corrections, but it makes the Z_c^+ search tractable since it reduces the number of $J/\psi(k)\pi(-k)$ and $D(k)\bar{D}^*(-k)$ states in the considered energy range.

Interpolating fields

We implement altogether 18 interpolators with $I^G = 1^+$, $J^{PC} = 1^{+-}$ and total momentum zero (using the irreducible representation T_1^{+-} of the lattice symmetry group O_h). The first fourteen interpolators $\mathcal{O}^{M_1 M_2}$ are expected to couple well with the two-meson states (2), while the last four are the diquark-antidiquark interpolators \mathcal{O}^{4q} with structure $[\bar{c}\bar{d}]_{3_c}[cu]_{\bar{3}_c}$

$$\begin{aligned}
\mathcal{O}_1 &= \mathcal{O}_1^{\psi(0)\pi(0)} = \bar{c}\gamma_i c(0) \bar{d}\gamma_5 u(0), \\
\mathcal{O}_2 &= \mathcal{O}_2^{\psi(0)\pi(0)} = \bar{c}\gamma_i \gamma_t c(0) \bar{d}\gamma_5 u(0), \\
\mathcal{O}_3 &= \mathcal{O}_3^{\psi(0)\pi(0)} = \bar{c} \overleftarrow{\nabla}_j \gamma_i \overrightarrow{\nabla}_j c(0) \bar{d}\gamma_5 u(0), \\
\mathcal{O}_4 &= \mathcal{O}_4^{\psi(0)\pi(0)} = \bar{c} \overleftarrow{\nabla}_j \gamma_i \gamma_t \overrightarrow{\nabla}_j c(0) \bar{d}\gamma_5 u(0), \\
\mathcal{O}_5 &= \mathcal{O}_5^{\psi(0)\pi(0)} = |\epsilon_{ijk}| |\epsilon_{klm}| \bar{c}\gamma_j \overleftarrow{\nabla}_l \overrightarrow{\nabla}_m c(0) \bar{d}\gamma_5 u(0), \\
\mathcal{O}_6 &= \mathcal{O}_6^{\psi(0)\pi(0)} = |\epsilon_{ijk}| |\epsilon_{klm}| \bar{c}\gamma_t \gamma_j \overleftarrow{\nabla}_l \overrightarrow{\nabla}_m c(0) \bar{d}\gamma_5 u(0), \\
\mathcal{O}_7 &= \mathcal{O}_7^{\psi(0)\pi(0)} = R_{ijk} Q_{klm} \bar{c}\gamma_j \overleftarrow{\nabla}_l \overrightarrow{\nabla}_m c \bar{d}\gamma_5 u(0), \\
\mathcal{O}_8 &= \mathcal{O}_8^{\psi(0)\pi(0)} = R_{ijk} Q_{klm} \bar{c}\gamma_t \gamma_j \overleftarrow{\nabla}_l \overrightarrow{\nabla}_m c \bar{d}\gamma_5 u(0). \\
\mathcal{O}_9 &= \mathcal{O}_9^{\psi(1)\pi(-1)} = \sum_{e_k = \pm e_{x,y,z}} \bar{c}\gamma_i c(e_k) \bar{d}\gamma_5 u(-e_k), \\
\mathcal{O}_{10} &= \mathcal{O}_{10}^{n_c(0)\rho(0)} = \bar{c}\gamma_5 c(0) \bar{d}\gamma_i u(0), \\
\mathcal{O}_{11} &= \mathcal{O}_{11}^{D(0)D^*(0)} = \bar{c}\gamma_5 u(0) \bar{d}\gamma_i c(0) + \{\gamma_5 \leftrightarrow \gamma_i\}, \\
\mathcal{O}_{12} &= \mathcal{O}_{12}^{D(0)D^*(0)} = \bar{c}\gamma_5 \gamma_t u(0) \bar{d}\gamma_i \gamma_t c(0) + \{\gamma_5 \leftrightarrow \gamma_i\}, \\
\mathcal{O}_{13} &= \mathcal{O}_{13}^{D(1)D^*(-1)} = \sum_{e_k = \pm e_{x,y,z}} \bar{c}\gamma_5 u(e_k) \bar{d}\gamma_i c(-e_k) + \{\gamma_5 \leftrightarrow \gamma_i\}, \\
\mathcal{O}_{14} &= \mathcal{O}_{14}^{D^*(0)D^*(0)} = \epsilon_{ijk} \bar{c}\gamma_j u(0) \bar{d}\gamma_k c(0),
\end{aligned} \tag{6}$$

$$\begin{aligned}
\mathcal{O}_{15} &= \mathcal{O}_1^{4q} = N_L^3 \epsilon_{abc} \epsilon_{ab'c'} (\bar{c}_b C \gamma_5 \bar{d}_c c_{b'} \gamma_i C u_{c'} - \bar{c}_b C \gamma_i \bar{d}_c c_{b'} \gamma_5 C u_{c'}), \\
\mathcal{O}_{16} &= \mathcal{O}_2^{4q} = N_L^3 \epsilon_{abc} \epsilon_{ab'c'} (\bar{c}_b C \bar{d}_c c_{b'} \gamma_i \gamma_5 C u_{c'} - \bar{c}_b C \gamma_i \gamma_5 \bar{d}_c c_{b'} C u_{c'}), \\
\mathcal{O}_{17} &= \mathcal{O}_3^{4q} = \mathcal{O}_1^{4q} (N_v = 32), \\
\mathcal{O}_{18} &= \mathcal{O}_4^{4q} = \mathcal{O}_2^{4q} (N_v = 32).
\end{aligned}$$

Here i denotes the polarisation and the correlation matrix is averaged over $i = x, y, z$. The Q_{klm} are taken from [16] and R_{ijk} from [33].

The momenta are projected separately for each meson $M_1(\mathbf{k})M_2(-\mathbf{k})$ in $O^{M_1 M_2}$

$$M(\mathbf{k}) : \quad \bar{q}_1 \Gamma q_2(\mathbf{k}) \equiv \sum_x e^{i2\pi \mathbf{k}x/L} q_1(x, t) \Gamma q_2(x, t) \quad \mathbf{k} \in \mathbb{N}^3 \quad (7)$$

The momentum in \mathcal{O}^{4q} is projected to zero

$$\mathcal{O}^{4q} = N_L^3 \sum_x \bar{c}_b(x, t) \Gamma_1 \bar{d}_c(x, t) c_{b'}(x, t) \Gamma_2 u_{c'}(x, t) \quad (8)$$

and a factor N_L^3 is included to achieve similar normalization as for $O^{M_1 M_2}$. The \mathcal{O}^{4q} are implemented as

$$\tilde{\mathcal{O}}^{4q} = N_L^3 \sum_{x_1} \bar{c}_b(x_1, t) \Gamma_1 \bar{d}_c(x_1, t) \sum_{x_2} c_{b'}(x_2, t) \Gamma_2 u_{c'}(x_2, t) \quad (9)$$

which reduces to \mathcal{O}^{4q} after the average over gauge configurations, where the gauge is not fixed. We verified that $\langle \tilde{\mathcal{O}}^{4q} | \tilde{\mathcal{O}}^{4q\dagger} \rangle \simeq \langle \mathcal{O}^{4q} | \mathcal{O}^{4q\dagger} \rangle$.

All quark fields in (6) are smeared $q \equiv \sum_{k=1}^{N_v} v^{(k)} v^{(k)\dagger} q_{point}$ according to the distillation method [34, 16]. We employ $N_v = 64$ Laplacian eigenvectors for all interpolators with exception of $\mathcal{O}_{3,4}^{4q}$ where the smearing with $N_v = 32$ is used.

Eight interpolators $\mathcal{O}_{1,\dots,8}^{\psi(0)\pi(0)}$ are implemented in order to allow the reliable extraction of two-meson states $\psi(0)\pi(0)$ with $\psi = J/\psi, \psi(2S), \psi(3770), \psi_3$. We verified for conventional charmonium that eight $\bar{c}c$ structures in $\mathcal{O}_{1,\dots,8}^{\psi\pi}$ lead to a reliable signal for these four ψ 's after the diagonalization of the 8×8 correlation matrix. The first six $\bar{c}c$ structures were employed already in [16], while $\mathcal{O}_{7,8}^{\psi\pi}$ were added to enhance overlap with ψ_3 [33]. The ψ_3 denotes the charmonium with $J^{PC} = 3^{--}$ and appears in addition to 1^{--} states when charmonia are simulated using the irreducible representation T_1^{--} . This is a consequence of the broken rotational invariance on a lattice with finite lattice spacing, where the continuous symmetry group is reduced to O_h . In order to study the $J^{PC} = 1^{+-}$ channel in this work, we employ lattice interpolators that transform according to irreducible representation T_1^{+-} of O_h . This irreducible representation contains $J^{PC} = 1^{+-}$ states, but also the $\psi_3 \pi$ state with $J^{PC} = 3^{+-}$.

Wick contractions

The Wick contractions that appear in the correlation matrix (3) for interpolators (6) are drawn in Fig. 4. Our correlation matrix is averaged over every second t_{src} , and is based on the Wick contractions in Fig. 4a, as explained in the main text.

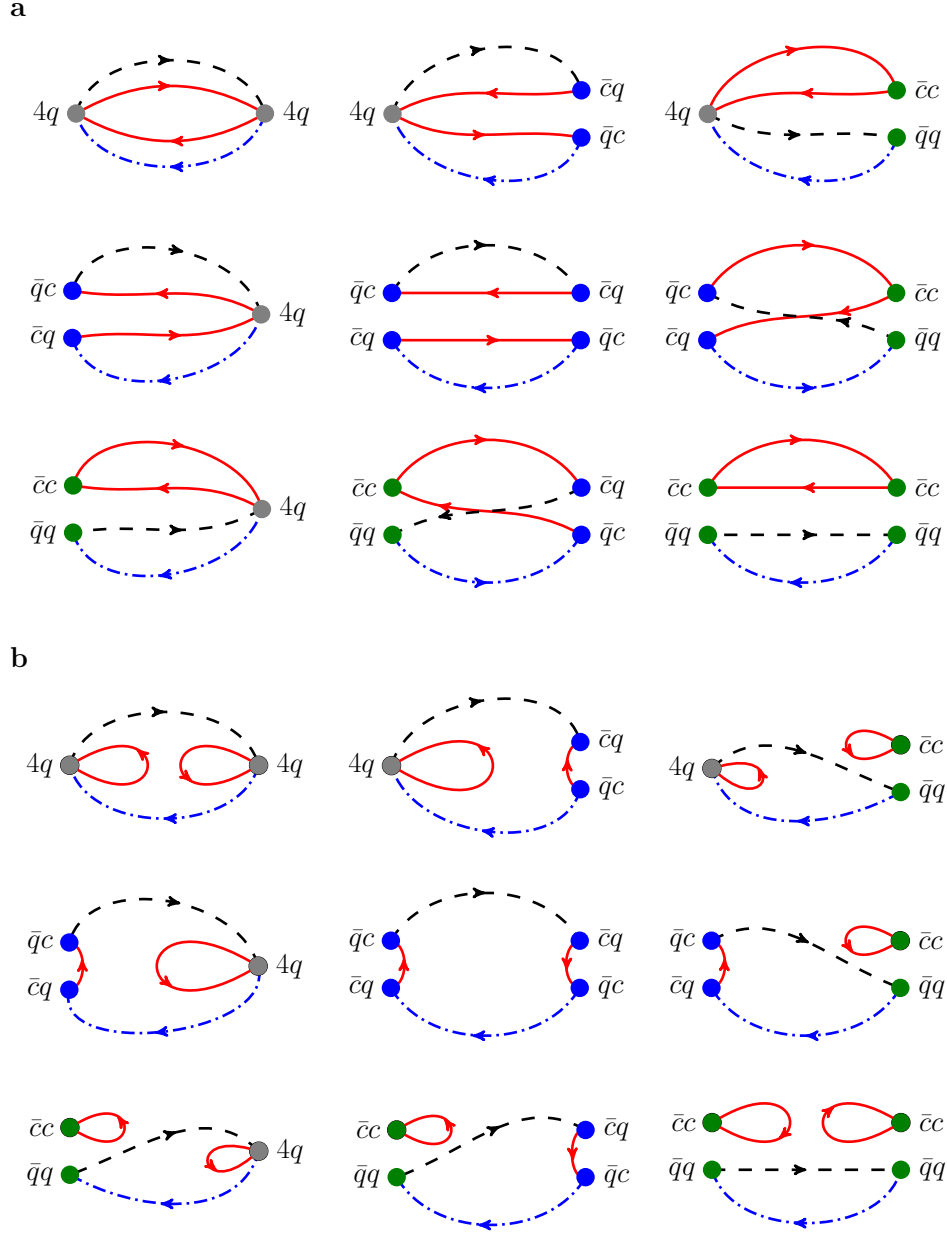


Figure 4: **Wick contractions.** Wick contractions that enter the correlation matrix $C_{jk}(t)$ for the interpolators (6). A red solid line represents a c quark, a black dashed line represents u , and the blue dash-dotted line stands for d . **a** Nine diagrams where charm does not annihilate; **b** Nine diagrams where charm annihilates.

Overlaps $\langle \Omega | \mathcal{O}_j | n \rangle$ for all eigenstates

The overlaps $\langle \Omega | \mathcal{O}_j | n \rangle$ for the eleven lowest eigenstates to all employed interpolators are provided in Fig. 5. They show which Fock components are important for various eigenstates.

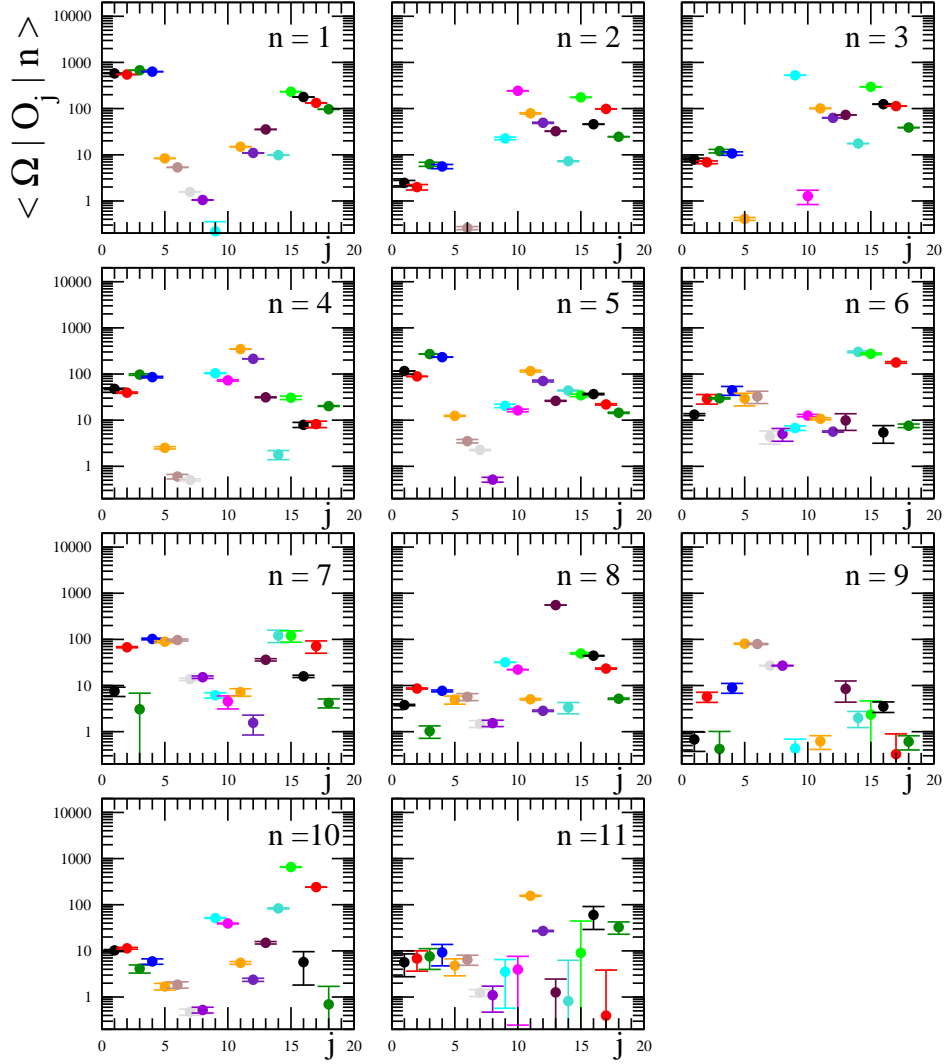


Figure 5: **Full spectrum operator composition.** These overlaps $\langle \Omega | \mathcal{O}_j | n \rangle$ (4) show the matrix elements of interpolators \mathcal{O}_j between the vacuum $\langle \Omega |$ and the physical eigenstate $|n\rangle$ on the lattice. Levels $n = 1, \dots, 11$ are ordered from lowest to highest E_n . The horizontal axis denotes $j = 1, \dots, 18$ corresponding to interpolator \mathcal{O}_j (6).